Numerical Simulation of Three Dimensional Flow in a Centrifugal Fan

WANG CAN-XING, SUI XI

Department of Mechanics

Zhejiang University

No.38, Zheda Road, Hangzhou City, Zhejiang Province, 310027

CHINA

Abstract: In this paper, a method of numerical simulation for the centrifugal fan was developed. A multi-regions system is employed to simulate the flow of the centrifugal fan, and the different grid structure is used to different regions. The RNG $k - \varepsilon$ turbulence model is used in simulation. Some important flow features have found from the results of simulation. The results of experiment show that the method of simulation is reliable.

Key-Words: Centrifugal Fan, Simulation, Flow, Turbulence Model, Grid

1 Introduction

In recent years, many kinds of numerical simulation for centrifugal fan have been developed, most of them are respectively simulating the flow field in impeller or scroll, but the flow field in the centrifugal fan is very complex and these conventional methods can not consider that the dissymmetry of scroll affects the internal flow of impeller, so it is difficult to give the proper boundary conditions, the results of the simulation are not accordant with the experiment. If the numerical simulation is based on the whole flow field in centrifugal fan, the boundary conditions can be suitably set up, and the influence of the dissymmetry of scroll on the flow in impeller will be found also. In this paper a method about numerical simulation of three-dimensional quasi-steady flow in a centrifugal fan is constituted by choosing the appropriate simulation method, some flow features will be analyzed.

The centrifugal fan with backward blade is composed of three components, that is, the inlet, the impeller and the scroll, as shown in figure 1.
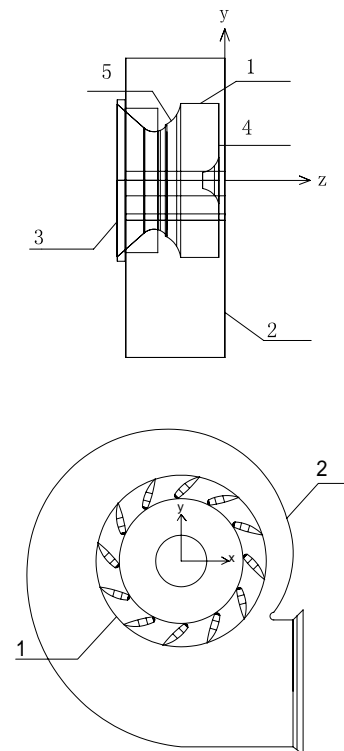

Fig.1   the sketch of the centrifugal fan

1   impeller 2   scroll 3   inlet 4   back plate 5   shroud

2 The Model of Numerical Simulation

2.1 The Model of the Centrifugal Fan

2.2 The Governing Equations

The governing equations for steady, three-dimensional and incompressible mean-flow in centrifugal fan can be written as following in Cartesian coordinates.

$$\text{div}\, u = 0 \tag{1}$$

$$\frac{\partial u}{\partial t} + \text{div}\,(u\mathbf{u}) = -\frac{1}{\rho}\frac{\partial p}{\partial x} + v\,\text{div}\,(\text{grad}\, u) \tag{2}$$

$$\frac{\partial v}{\partial t} + \text{div}\,(v\mathbf{u}) = -\frac{1}{\rho}\frac{\partial p}{\partial y} + v\,\text{div}\,(\text{grad}\, v) \tag{3}$$

$$\frac{\partial w}{\partial t} + \text{div}\,\rho\,(w\mathbf{u}) = -\frac{1}{\rho}\frac{\partial p}{\partial z} + v\,\text{div}\,(\text{grad}\, w) \tag{4}$$

Here, u, v, w are the fluid velocity components, ρ is the fluid density and v is the dynamic viscosity.

2.3 Turbulent Model

Because of its stability, economy and the precise of the computation the standard $k-\varepsilon$ turbulence model is widely used in simulation of flow, but it assumes that the turbulence is isotropic, it is not suitable for rotational flow. So the RNG $k-\varepsilon$ model and the Realizable $k-\varepsilon$ model, which are the improved $k-\varepsilon$ models, are developed. In this paper, the RNG $k-\varepsilon$ model is selected, as shown in equations (5) and (6), it has two advantages, firstly, the rotational flow are taken into consideration by the modified viscosity, μ_{eff}, secondly, the deformation of the mean flow, E_{ij}, is reflected by the accessorial item $C_{1\varepsilon}^{*}$ in the equation (6). Thus the RNG $k-\varepsilon$ model is good at dealing with the flow which has high deformation and the large curvature of the stream line, such as the internal flow in centrifugal fan.

$$\frac{\partial(\rho k)}{\partial t} + \frac{\partial(\rho k u_i)}{\partial x_i} = \frac{\partial}{\partial x_j}\left[\alpha_k \mu_{eff}\frac{\partial k}{\partial x_j}\right] + G_k + \rho\varepsilon \tag{5}$$

$$\frac{\partial(\rho\varepsilon)}{\partial t} + \frac{\partial(\rho\varepsilon u_i)}{\partial x_i} = \frac{\partial}{\partial x_j}\left[\alpha_k \mu_{eff}\frac{\partial\varepsilon}{\partial x_j}\right] + \frac{C_{1\varepsilon}^{*}\varepsilon}{k}G_k - C_{2\varepsilon}\rho\frac{\varepsilon^2}{k} \tag{6}$$

$$\mu_{eff} = \mu + \mu_t \tag{7}$$

$$\mu_t = \rho C_\mu \frac{k^2}{\varepsilon} \tag{8}$$

$$C_\mu = 0.0845, \alpha_k = \alpha_\varepsilon = 1.39 \tag{9}$$

$$C_{1\varepsilon}^{*} = C_{1\varepsilon} - \frac{\eta(1-\eta/\eta_0)}{1+\beta\eta^3} \tag{10}$$

$$\eta = \left(2E_{ij}gE_{ij}\right)^{1/2}\frac{k}{\varepsilon} \tag{11}$$

$$E_{ij} = \frac{1}{2}\left(\frac{\partial u_i}{\partial x_j} + \frac{\partial u_j}{\partial x_i}\right) \tag{12}$$

$$\eta_0 = 4.377, \beta = 0.012 \tag{13}$$

Here k is turbulence kinetic energy and ε is the turbulence dissipation rate, u_i and u_j are velocity components.

Because the turbulence is not well development near the wall zone, the standard wall function is used instead of original turbulence model. The governing equations are dispersed by the second order upwind difference format, because this format is more precise and the flow phenomenon in the centrifugal fan, for example, the separation of the boundary layer and the jet-wake flow in impeller are more obviously, under the same grid number.

2.3 The Partition of the Grid

For giving better boundary condition, there are two additional pipes which are combined with the inlet and the scroll respectively, see figure 2. The length of the pipes is not specified, but the length must be enough long to ensure that the flow in the pipes are fully developed.
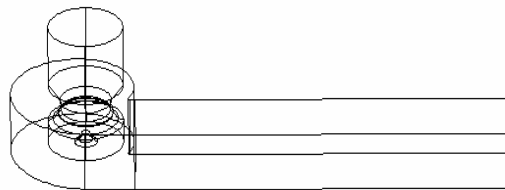

Fig.2 the structure in simulation

2

According to the difference of the flow in centrifugal fan, the numerical zones is divided into four regions, the inlet, the impeller, the scroll and the pipe region, these regions are meshed respectively. Because the flow in the additional pipes, which are combined with the inlet and scroll, are relatively simple, the size of the grid in these two parts is large, but in the impeller and the scroll, the flow is much more complex and the rough grid will result in the inaccurate computation. The grid structure affects sharply the numerical precision and computing efficiency the non-structure grid is used in simulation, table 1 shows the grid type for every region and the number of grid. The boundary conditions are velocity in inlet, the pressure in outlet, and non-slip on wall. At the inlet and outlet, the turbulence parameters are turbulence intensity and hydraulic diameter.

Table 1

Region	Grid type	Grid number
Inlet pipe	Mixed grid	278304
impeller	Tetrahedral grid	1692006
scroll	Tetrahedral grid	806543
Outlet pipe	Rectangular grid	231000
Total grid	Mixed grid	3007853

3 The Numerical Result and the Discuss

The simulation in this paper is for a fan widely used in industry, and the rotation speed is 580 rpm. Figure 3 is the grey-scale map of the relative velocity magnitude in the plane which is close to the shroud. There are some low velocity zones near the suction surfaces. It is the boundary layer separation phenomenon actually. Figure 4 shows the relative stream lines in the flow passage of the impeller. The backflow and the vortex can be seen obviously.

It can be seen from Fig.3 that the separation of boundary layer does not exist in each impeller flow passage, for example, on the left of the impeller, there is no separation of boundary layer. It is caused by the dissymmetry of the scroll which makes the dissymmetrical distribution of the velocity and static pressure. Fig.5 is the grey scale map of the static pressure in the plane which is close to the shroud. It can be seen from Fig.5 that in the flow passage of impeller where the boundary layer does not separate from the suction surface, the variety of the static pressure centralizes to the edge region of the suction surface, but in the flow passage where the boundary layer separates, the static pressure varies obviously from the middle of the suction surface.
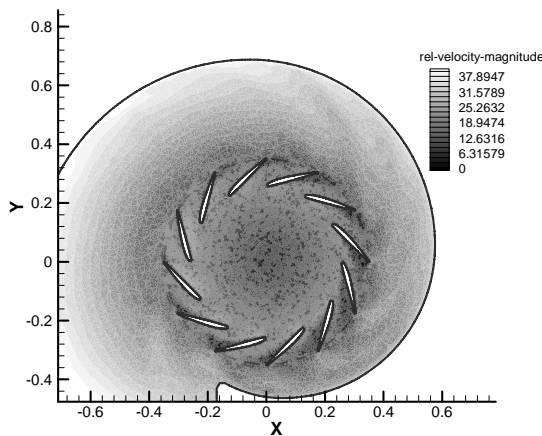
Fig.3 the relative velocity magnitude
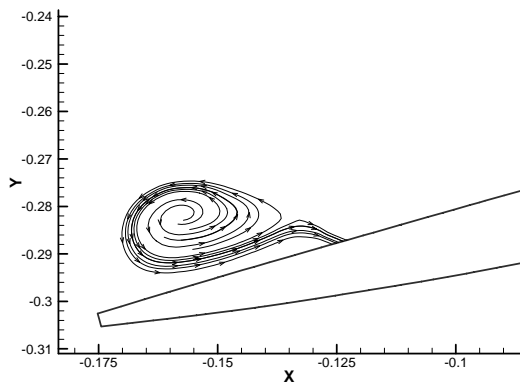(x-y)-plane view at z=-0.18m

3

Fig.4 the relative stream lines near the suction surface

(x-y)-plane view at z=-0.18m

Fig.6 is the relative velocity magnitude of a plane which is close to the shroud. The relative velocity magnitude of each flow passage of impeller
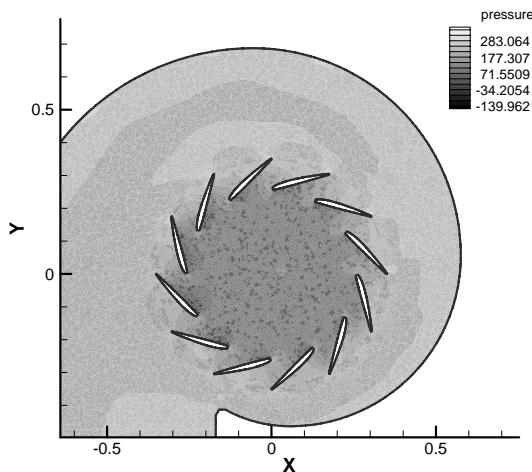
plate. The status of the flow is much better and there is no boundary layer separation phenomenon. From the comparison of the Fig.7 and Fig.11 it can be seen that the energy loss of the centrifugal fan is concentrated on the zone which is close to the shroud. The relative velocity magnitude at the inlet of each flow passage in Fig.7 is more symmetrical than that in Fig.6. This is one of the reasons why there is no boundary layer separation phenomenon in Fig.7.

Fig.8 and Fig.9 are shown respectively the static pressure and the velocity magnitude in the plane which is close to the back plate. From Fig.8 it can be seen that the variety of the static pressure centralizes to the edge region of the suction surface. This is another reason why there is no boundary layer separation phenomenon. The jet-wake flow can be seen in Fig.9
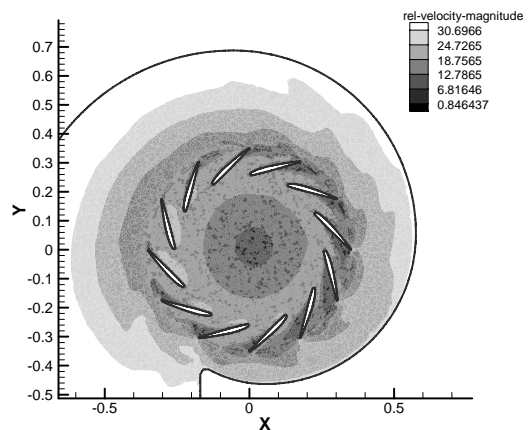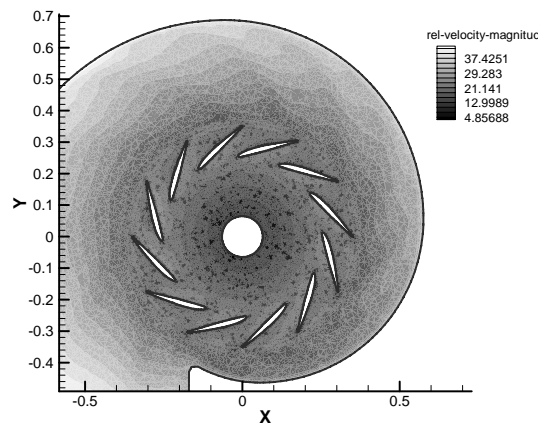

Fig.5 the static pressure

(x-y)-plane view at z=-0.18m

Fig.6 the relative velocity magnitude

(x-y)-plane view at z=-0.18m

Fig.7 the relative velocity magnitude

is also not the same. At the inlet of the flow passage in which the boundary layer separates from the suction surface, the relative velocity magnitude is small. And at the inlet of the flow passage in which the boundary layer does not separate, the relative velocity magnitude is large. The difference of the relative velocity magnitude is the reason of the dissymmetrical distribution of the boundary separation phenomenon. Fig.7 is the relative velocity magnitude in the plane which is close to the back
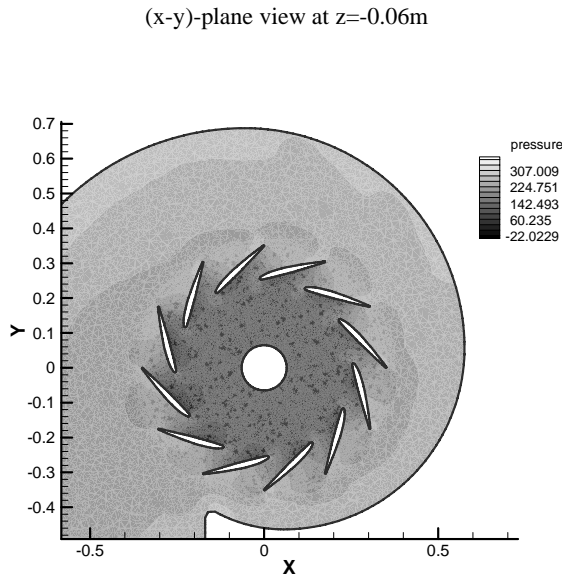
(x-y)-plane view at z=-0.06m

Fig.8 the static pressure
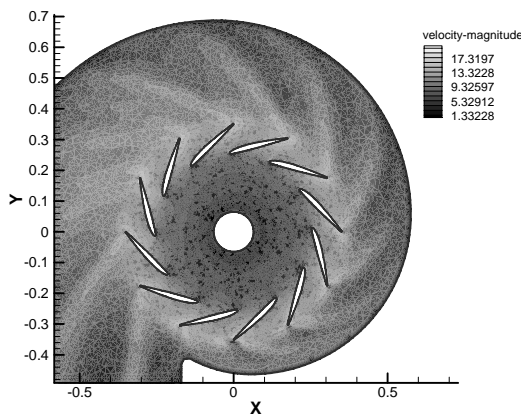
(x-y)-plane view at z=-0.06m

Fig.9 the velocity magnitude

(x-y)-plane view at z=-0.06m

Table 2 is the comparison of experimental static pressure and computational static pressure under the different rotation speed. It is shown that the computational results are coincident with the experimental results very well. So the computational model in this paper is suitable for the simulation of the centrifugal fan.

Table 2

Rotation speed (rpm)	580	730	960	1450
Experimental static pressure (ESP) (Pa)	189.5	300.6	513.6	1166.3
Computational static pressure (CSP) (Pa)	175.0	316.5	548.4	1257.0
CSP/ESP (%)	92.3	105.3	106.8	107.8
Volume flow rate (m^3/h)	1.8698	2.370	3.1203	4.7076

The gird is very important for obtaining an accurate result. For example, if the size of the grid in the impeller region is large, the separation of the boundary layer is not obvious, because in this region, the flow field is very complex, the velocity and the pressure vary rapidly. On the contrary, if the size of the grid is too small, the computational efficiency will be low and the solution is hard to be converged. The difference scheme is also very important, if the difference is first order precise, the jet-wake flow can not be found in the flow field. To get a better result, the first order format is used in the computation at first. When the solution is converged, the second order format is selected to the continuous computation.

4 The Conclusion

Some phenomena of the flow in the centrifugal fan are found by the simulation. For example, the boundary layer separation, the dissymmetrical distribution of the velocity and the static pressure, the jet-wake flow and the different distribution of the pressure and the velocity in the two planes one of which is near the shroud and the other one is near the back plate. The flow in the centrifugal fan is complex and the dissymmetry of scroll will affect the flow in impeller, so the simulation only in the impeller or in the scroll is inaccurate, and the results of simulation are usually different with the experimental results. Only the simulation of the whole centrifugal fan

5

could get the accurate results and can provide the guidance for the improvement and design of the centrifugal fan.

Reference

[1] Shen Tian-yao, *The Theoretical Basis of the Flow in the Centrifugal Impeller*, Zhejiang University Press, 1986. (In Chinese)

[2] Hou Shu-qiang, Wang Can-xing, Lin Jianzhong, Review on the Numerical Simulation of Internal Flow in the Rotating Fluid Machinery, *Fluid machinery,* 2005, Vol.33, pp.30-34. (In Chinese)

[3] Li Xin-hong, He Hui-wei, Gong Wu-qi, Huang Shu-juan, Numerical Analysis of Whole Steady Flow Field for a Centrifugal Fan, *The Transaction of Engineering Thermal-Physics*, 2002, Vol. 23, No.3, pp.453-456. (In Chinese)

[4] Zhao Yu, Song Li, He Wen-qi, Numerical Simulation of Flow Field for a Whole Centrifugal Fan and Analysis of the Effects of Blade Inlet Angle and Impeller Gap, *HVAC&R RESEARCH*, 2005, No.11, pp.263-283. (In Chinese)

[5] Yang Hong-wei, Zhou Ping, Xiao Zhe-qiang, Three Dimensional Transient Computation of Flow Field in Centrifugal Fan, *Journal of Central South University of Technology*, 1999, Vol.30, No.1, pp.37-40. (In Chinese)

[6] Lin Sheam-chyun, Huang Chia-lieh, An Integrated Experimental and Numerical Study Fan, *Experimental Thermal and Fluid Science*, 2002, Vol.26, pp.421–434.

[7] D.V. Bhope, P.M. Padole, Experimental and Theoretical Analysis of Stresses, Noise and Flow in Centrifugal Fan Impeller, *Mechanism and Machine Theory*, 2004, Vol.39, pp.1257– 1271.

[8] Wan-Ho Jeon, A Numerical Study on the Effects of Design Parameters on the Performance and Noise of a Centrifugal Fan, *Journal of sound and vibration*, 2003, Vol.265,pp.221-230.

[9] Zhang, M.J, M.J. Pomfret, C.M. Wong, Three-Dimensional Viscous Flow Simulation in a Backswept Centrifugal Impeller at the Design Point, *Computers & Fluids*, 1996, Vol.25, pp.497-507.

[10] Miner, S.M, Evaluation of Blade Passage Analysis Using Coarse Grids, *Journal of Fluids Engineering*, 2000, Vol.122, pp.345-348.